

# Assessment of Electromechanical Performance of Graphene-Reinforced Aluminum Nanocomposites for Energy Storage Solutions

Shashank Dubey<sup>1\*</sup>, Sandip Kumar Singh<sup>1</sup>, Himanshu Tiwari<sup>1</sup>

<sup>1</sup>Department of Mechanical Engineering, Veer Bahadur Singh Purvanchal University, Jaunpur, Uttar Pradesh, India 222003

\*Corresponding Author : Shashank Dubey

\*Email : [shashank.dubey001@gmail.com](mailto:shashank.dubey001@gmail.com) ORCID : 0009-0006-0729-4760

## ABSTRACT

Graphene insertion into aluminium matrix composites (AMCs) has demonstrated a great deal of promise for improving the electromechanical characteristics that are essential for energy storage applications. This work explores the electromechanical properties of aluminium nanocomposites reinforced with graphene, with a particular emphasis on the materials' conductivity, capacity for storing charge, and general appropriateness for applications in super capacitors and advanced batteries. Aluminium can be reinforced with graphene because of its superior mechanical strength, large surface area, and outstanding electrical conductivity. A range of fabrication techniques, including chemical reduction procedures and powder metallurgy, were utilized to attain the best possible dispersion of graphene in the aluminium matrix. Optimising the interfacial connection between graphene and aluminium resulted in improved electromechanical performance and efficient load transmission. The results of this study highlight the potential contribution of aluminium nanocomposites reinforced with graphene to the advancement of energy storage technologies. Future research will concentrate on understanding the fundamental principles that control these materials' electromechanical behaviour and investigating the materials' long-term stability and scalability for commercial uses.

**Keywords:** Reduced graphene oxide, Ball milling. Metal matrix composite, Surface morphology

## INTRODUCTION

The need for advanced energy storage systems is growing, which has accelerated the development of novel materials with exceptional electrical and mechanical capabilities. Because of its remarkable mechanical, thermal, and electrical properties, graphene a single sheet of carbon atoms organized in a two-dimensional lattice has become a suitable reinforcement material for aluminium matrix composites (AMCs) [1]. Graphene is incorporated into aluminum to increase both its mechanical and electromechanical properties [2]. As a result, these nanocomposites have potential applications in supercapacitors and batteries. Graphene-reinforced aluminum nanocomposites (GRANs) offer a special combination of high strength, low weight, and superior electrical conductivity for energy storage applications [3-8]. Nevertheless, several obstacles must be overcome for graphene to integrate into the aluminum matrix successfully. These include problems with agglomeration, interfacial bonding, and uniform graphene dispersion. These elements have the potential to greatly affect the nanocomposite's overall performance, so a careful evaluation of its electromechanical characteristics is required [9]. The objective of this study is to conduct a thorough assessment of the electromechanical performance of aluminium nanocomposites reinforced with graphene, with a particular emphasis on their mechanical integrity, conductivity, and charge storage capacity. This work aims to provide a thorough understanding of the connections between microstructural properties and electromechanical performance by examining several production methods and optimizing graphene content [10]. The results will open the door for the creation of high-performing energy storage systems and the subsequent generation of energy systems that are both lightweight and effective. The surface morphology of nanocomposites is a critical factor influencing their mechanical and thermal properties. The efficiency of load transmission and overall performance is significantly impacted by the distribution, dispersion, and interfacial interactions between the matrix and the reinforcing phase. Therefore, a comparative analysis of the surface morphology in aluminium matrix graphene nanocomposites synthesized by the wet method and ball milling method is essential for understanding the effects of different fabrication techniques on the final composite structure [11].

In this paper, we report a comprehensive comparative examination of the surface morphology in wet- and ball-milled-produced aluminium matrix graphene nanocomposites. We intend to clarify the changes in surface morphology arising from the dispersion and distribution of graphene nanoparticles during the production process by studying the surface properties using scanning electron microscopy (SEM), EDS, and FTIR

## MATERIAL AND EXPERIMENTAL METHODS

### Materials

Graphite flakes (350 mesh size, purchased from Alfa Aesar) was used to synthesize graphene oxide (GO). Sulphuric acid ( $H_2SO_4$ , 98%), potassium permanganate ( $KMnO_4$ , 99.9%), hydrogen peroxide ( $H_2O_2$ , 30%) were purchased from alpha aesar and used as received.  $NaNO_3$  and aluminium powder was purchased from Huntsman Advanced Material, India and used as received. Distilled water and ethanol were used throughout the sample preparation.

### Synthesis of reduced graphene oxide (RGO)

Fig 1 shows the process of making graphene oxide generally involves the following steps:

1. Preparation of graphene oxide: Graphene oxide was typically prepared by the oxidation of graphite (5g) mixed with 2.5g  $NaNO_3$  using a strong oxidizing agent such as potassium permanganate (15g very slowly) mixed with 115 mL concentrated  $H_2SO_4$ . This process introduces oxygen-containing functional groups onto the surface of graphene, making it hydrophilic. The mixture was stirred for 1 h at  $35^\circ C$  after stirring 140mL of DI water and 5 ml of  $H_2O_2$  was added to the solution and stirred for 3h [12].
2. Reduction of graphene oxide: The reduction of graphene oxide is necessary to remove the oxygen-containing functional groups and restore the  $sp^2$  carbon-carbon bonding of graphene. This can be achieved through the mixing of graphene oxide and a reducing agent (sodium borohydride 2g) the graphene oxide and reducing agent are mixed in a solvent ethanol. The mixture is then stirred to ensure that the graphene oxide is well dispersed. The mixture is heated, typically at temperatures between  $70^\circ C$  to  $100^\circ C$ , to initiate the reduction reaction [13].
3. Exfoliation of graphene: The reduced graphene oxide can then be exfoliated into individual graphene sheets through mechanical shearing for 2 h, mechanical stirring break apart the graphene oxide flakes and disperse the resulting graphene sheets into a solvent.
4. Purification of graphene: The graphene sheets may contain impurities such as residual oxidizing agents, untreated graphene oxide, or metallic catalysts used during synthesis. Therefore, the resulting graphene must be purified using DI water and ethanol many times and filtered and dried at  $70^\circ C$  [14].

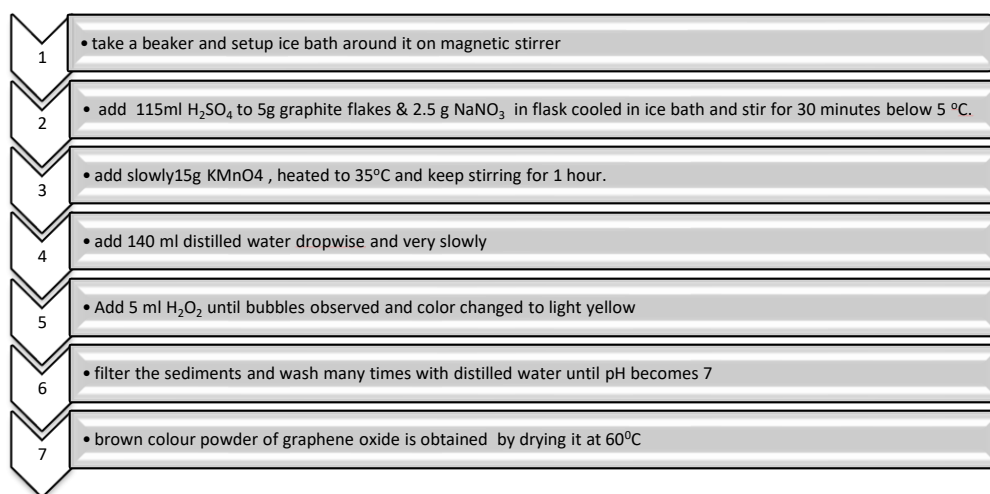


Fig. 1 Illustration of detailed processing of GO

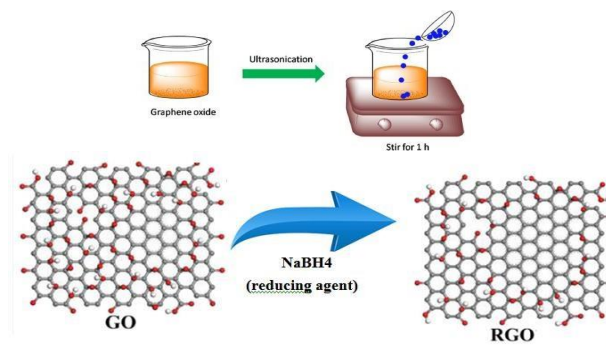


Fig. 2 Reduction of GO to RGO

**Fabrication of Al-RGO composite**

In this research work powder metallurgy method and wet method were used to prepare Al-xRGO nanocomposite material (where x=%wt of graphene). In the ball milling technique different %wt of reduced graphene oxide powder was mixed with Al powder in a ball mill at room temperature for 5h using a steel ball and ball to powder ratio was kept 20:1, to remove the impurities the samples were dried further at 800C for 12h.while in wet method different %wt of reduced graphene oxide powder was mixed with 20 mL ethanol for 1 hr ultrasonication and separately dispersion of Al powder (10g) with 20 ml ethanol for 1 hr ultrasonication. Then there is a drop wise addition of RGO slurry in Al slurry as shown in fig 3. After 1 hr of ultrasonication, the sample was filtered and dried at 80°C for 6hr [15].

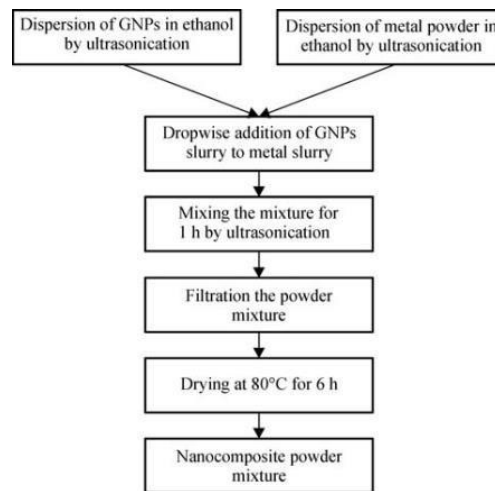


Fig. 3 Illustration of detailed fabrication of Al-RGO composite by wet method

The composite nanomaterials were preheated to relieve the accumulated stress during milling process. A satisfactory compaction of powders is ensured by this stress-relieving technique. Uniaxial die pressing is carried out for both the samples generated by the ball milling method (sample 1 GrAIB) and the wet method (sample 2 GrAIW) using a 16-mm-diameter hardened die steel. Green compacts' cylindrical billets are successfully made utilizing uniaxial die pressing for 30 minutes at 600 MPa of pressure. These green compacts are sintered for one hour at 600 °C in an inert argon environment within a heating tube chamber. High-resolution Transmission Electron Microscope (TEM, Jeol JEM 2100) and SEM with an Energy-Dispersive Spectroscopy (EDS) detector are used to study the morphology of the specimens.

According to ASTM E384 Standard, a micro Vickers hardness tester (Model: FMV-1) is used to measure the specimen's hardness under a 0.1 kg force for 10 seconds. Each specimen's surface has three measurements taken at random intervals, which are averaged. Use of the pin-on-disc tester (TR-20LE-PHM 400 DUCOM) to measure wear behaviour under dry sliding conditions at room temperature. According to ASTM G99 Standard, typical spherical specimens with a diameter of 10 mm are moved at a speed of 400 RPM across a distance of 402.12 m under loads of 20 N and 30 N.

## Results and Discussions

### Characterization

Figs.4 and 5 show the Scanning electron microscopy (SEM) & EDS of pure grapheme which is prepared by the modified hummer's method EDS graph shows 99.7% carbon

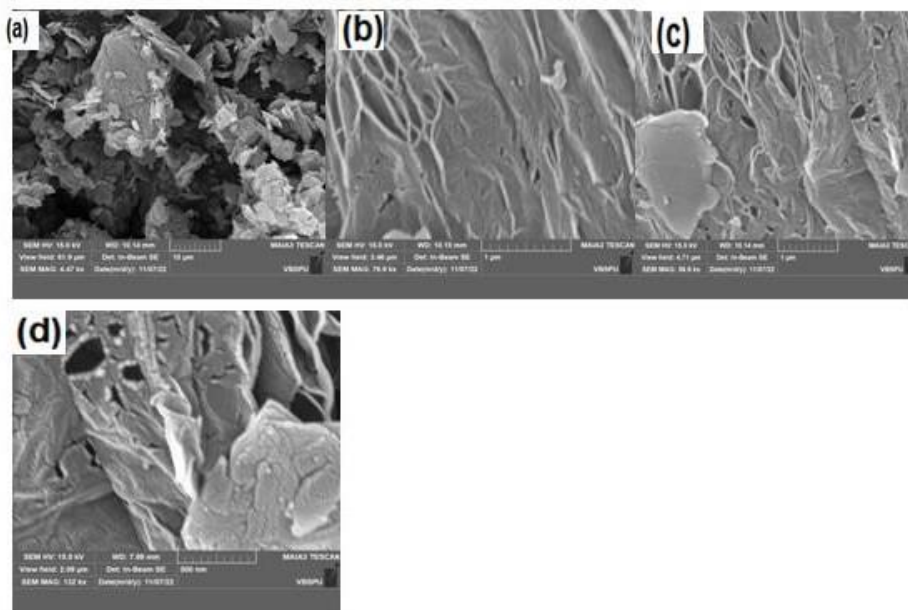


Fig. 4. Scanning electron microscopy (SEM): (a-d) of pure grapheme



Fig. 5. EDS of pure grapheme

Figs.6 and 7 show the morphology structure of Al-xRGO composite material powder (2%wt) after the wet mixing process. RGO sheets are observed on Al powder particles in composite, curled and wrinkled RGO sheets have covered the surfaces of Al powders, which is seen in the magnified SEMImage [16].

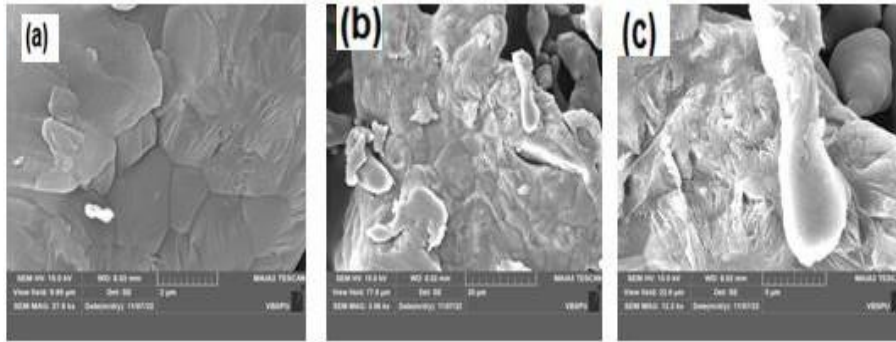


Fig.6.SEM image: (a-c) of Al-RGO nanocomposite material by wet method



Fig.7. EDS of AL+2%wt RGO by the wet method.

This result can lead to the efficient reinforcing effect of graphene in aluminium. The SEM images of AMC powders reinforced with graphene sheets indicated the distribution of the reinforcement phase on Al particles. However, the adsorption of graphene sheets on Al particles has been scarcely detected and graphene sheets have been mostly placed beside Al powders [17].

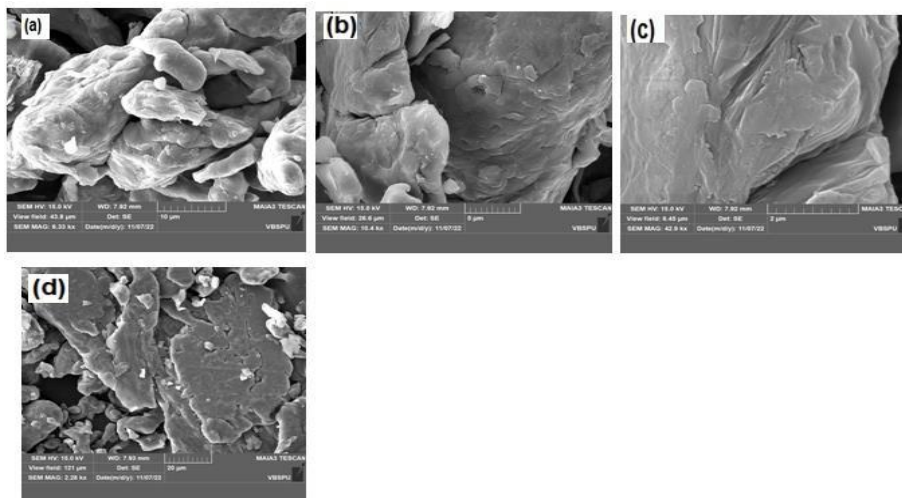


Fig.8.SEM image: (a-d) of Al- graphene nano material by ball milling.



Fig.9. EDS spectra of AL+2%wt graphene by ball milling.

The chemical bonds with various functional groups linked to the Al/Graphene nanocomposite material are confirmed by the FTIR study. The FTIR spectra of pure graphene are shown in Figure 10. The peak at 3910  $\text{cm}^{-1}$  in the graphene FTIR spectrum relates to the stretching vibration of free O-H produced by hydroxyl groups [18]. The low concentration of adsorbed water molecules in the graphene structure is shown by the weakness of this peak and the lack of additional peaks in the 3000–3700  $\text{cm}^{-1}$  range. The C=O stretching vibration of the carboxyl/carbonyl groups linked to the edges of RGO is what causes the peaks at 1238  $\text{cm}^{-1}$  and 1698  $\text{cm}^{-1}$ . The stretching vibration of aromatic C=C bonds, which represent carbons that are not functionalized during oxidation, is what gave rise to the peaks that occurred at 1647  $\text{cm}^{-1}$  and 1527  $\text{cm}^{-1}$ . The O-H stretching vibrations in hydroxyl groups and adsorbed water molecules are connected to the significant signal at 3500  $\text{cm}^{-1}$  in the RGO's FTIR spectrum [19].

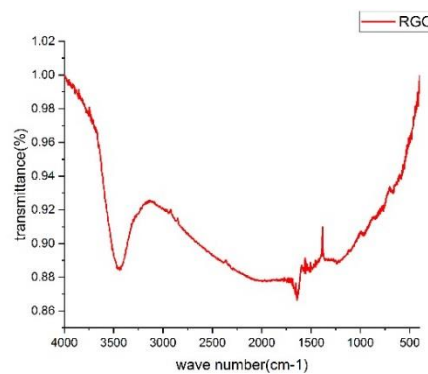


Fig.10. FT IR spectra of graphene.

Fig. 11(a & b) displays the FTIR spectra of the composite powders prepared by wet method and ball milling of Al and RGO powders. The spectra of the composite powder show the addition of two peaks at 1461  $\text{cm}^{-1}$  and 3418  $\text{cm}^{-1}$ , which are caused by the stretching vibrations of free O-H bonds and the bending vibrations of C-OH bonds, respectively [20].

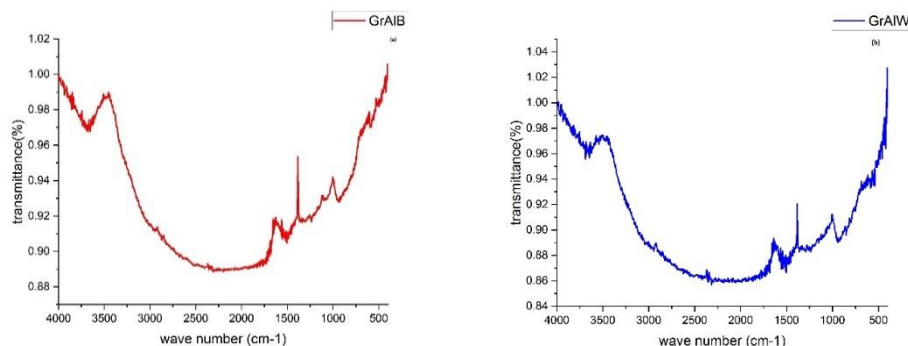


Fig.11. FT IR spectra of Al-RGO nanocomposite (a) by ball milling (b) by wet method.

Fig.12 demonstrates the hardness of nanocomposite material. The nanocomposite produced by the ballmilling process with 1.4% graphene reaches the maximum hardness of 105.4 HV; due to the strengthening effects of the particulates, the hardness increased in proportion with the increase in the

wt% of graphene added. Nano composite GrAlW has a lower hardness than nanocomposites made by the ball milling process. Ball milling may be helpful in creating flaws in the graphene sheets, which will increase the composite material's hardness [21]. The presence of graphene works as an interstitial atom in aluminium metal matrix composites, which will hamper the dislocation movement and reduce ductility, in accordance with Orowan looping mechanism. This is also clear from the TEM study, which shows that the population of graphene is uniform and dense. As a result of the Orowan looping process, also showed that the inclusion of graphene increased the hardness.

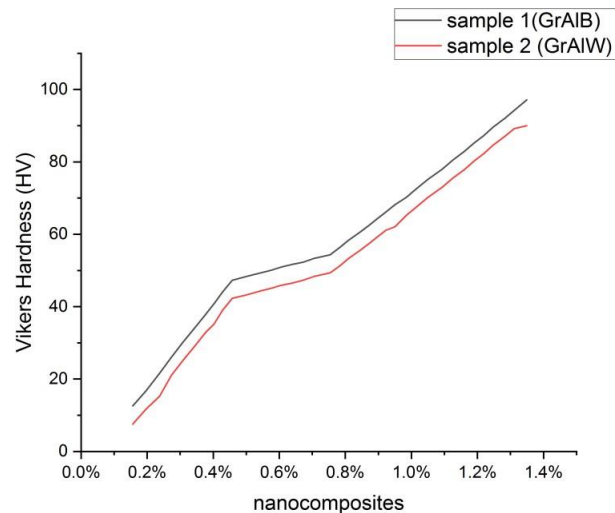


Fig.12. Micro Vickers hardness of nanocomposites

The wear rates under the varying load conditions for nanocomposites are shown in Fig.13. The increase in applied load leads to the increase in wear rate of the nanocomposites following the principle of Archard which states wear rate is directly proportional to the applied load. It should be noted that the increase in load gives better wear resistance to the composites due to the work hardening effect on the contact surface [22]. The work hardening is mainly due to the grain disintegration and dislocation builds up at the contact area. The nano composite material sample 2 GrAIW exhibited higher wear rate than the nanocomposite sample 1 GrAIB. Influence of adding graphene in the composites with respect to wear rate follows a decreasing trend. The effect of 0.75% graphene addition on the composites leads to a reduction in wear rate. When the graphene of 1% is added to the matrix, the wear rate is observed to increase. Further addition of the graphene beyond 0.75% does not have much influence on the wear rate. It is described that increased volume fraction of reinforcement enhances the wear resistance of the composite to a certain limit and exceeding beyond that causes clustering of particles [23].

It is also reported that the increased addition of nanoparticle will lead to the nanoparticle agglomeration, thereby leading to pores and subsequent detachment of conglomerated particles that are not bonded properly with the surface. The presence of graphene in the matrix acts as the barrier for the movement of dislocations, and the self-lubricating properties of graphene also attribute to the reduction in the wear rate of composites [24].



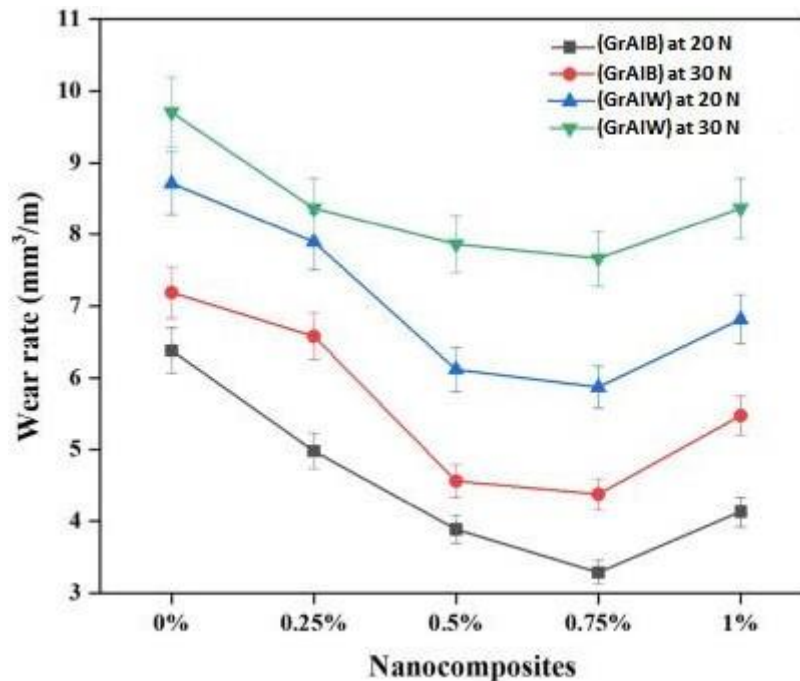


Fig.13. Wear rates of nanocomposites

## CONCLUSIONS

In this research paper, RGO was synthesized by a simplified Hummer's method and developed as low-cost, simple, and environmentally friendly without using toxic stabilizing, capping, or reducing agents to synthesize different RGO-based nanocomposites, including aluminium graphene nanocomposite material. The sample was studied and successfully characterized by using SEM, EDS, & FTIR, The SEM results suggest the uniform distribution of graphene nanoparticles in an aluminium metal matrix. The particle sizes obtained from these results are also supported by the earlier literature. The FTIR investigation validates the chemical bonding with diverse functional groups connected to the Al-RGO nanocomposite material. FTIR spectra of composite powders prepared by ball milling and wet method powders of aluminium and RGO show two additional peaks at  $1461\text{ cm}^{-1}$  and  $3418\text{ cm}^{-1}$ , which are brought about by the stretching vibrations of free O-H bonds and the bending vibrations of C-OH bonds, respectively. Therefore, it may be inferred that the mixing process to produce nanocomposites has a promising future if handled carefully.

This work is concentrated on the homogeneous distribution of reinforcement and its effects on the tribological properties. XRD result conclude that effective distribution of the reinforcement highly depends on the method of the reinforcement, which can be achieved by increasing the ball milling time. In conclusion, the wet method facilitates better dispersion and wetting of graphene nanoparticles, leading to a more homogeneous distribution on the aluminium matrix surface. On the other hand, the ball milling method subjects the nanoparticles to high mechanical forces, promoting the formation of graphene agglomerates and resulting in a less uniform distribution on the aluminium matrix surface. A maximum hardness of 105.4 HV is achieved with 1.4% wt. composition of graphene added in nanocomposite, increasing hardness and wear characteristics. Dislocations are prevented from moving by graphene, which also lubricates them. In order to produce lightweight, high-strength alloys, graphene reinforcements thus appear to be a suitable choice. Graphene with a 0.75% weight composition exhibited a lower wear rate even though it has a higher hardness. Beyond a graphene content of 0.75 percent, aggregation and brittleness are encouraged, which negatively impacts wear. Small amounts of graphene used in homogeneous reinforcement can significantly enhance an alloy's tribological characteristics.

## REFERENCES

- [1] K.B. Plantier, M.L. Pantoya, A.E. Gash, Combustion wave speeds of nanocomposite Al/Fe<sub>2</sub>O<sub>3</sub>: the effects of Fe<sub>2</sub>O<sub>3</sub> particle synthesis technique, *Combust. Flame* 140 (2005) 299–309.

- [2] Y. Liu, B. Gao, Z. Qiao, Y. Hu, W. Zheng, L. Zhang, Y. Zhou, G. Ji, G. Yang, Gramscale synthesis of graphene quantum dots from single carbon atoms growth via energetic material deflagration, *Chem. Mater.* 27 (2015) 4319–4327.
- [3] Saboori, A., Moheimani, S., Pavese, M., Badini, C. & Fino, P. New Nanocomposite Materials with Improved Mechanical Strength and Tailored Coefficient of Thermal Expansion for Electro-Packaging Applications. *Metals (Basel)*. 7, 536 (2017).
- [4] Tjong, S. Microstructural and mechanical characteristics of in situ metal matrix composites. *Mater. Sci. Eng. R Reports* 29, 49–113 (2000).
- [5] Liao, Z. et al. State-of-the-art of surface integrity in machining of metal matrix composites. *Int. J. Mach. Tools Manuf.* 143, 63–91 (2019).
- [6] Ma, Z. ., Tjong, S. . & Wang, Z. Cyclic and static creep behaviour of Al–Cu alloy composite reinforced with in-situ Al<sub>2</sub>O<sub>3</sub> and TiB<sub>2</sub> particulates. *Mater. Sci. Eng. A* 264, 177–187 (1999).
- [7] Tjong, S. Abrasion resistance of stainless-steel composites reinforced with hard TiB<sub>2</sub> particles. *Compos. Sci. Technol.* 60, 1141–1146 (2000).
- [8] Bai, G. et al. Tunable coefficient of thermal expansion of Cu-B/diamond composites prepared by gas pressure infiltration. *J. Alloys Compd.* 794, 473–481 (2019).
- [9] Dorri Moghadam, A. et al. Functional Metal Matrix Composites: Self-lubricating, Self-healing, and Nanocomposites-An Outlook. *JOM* 66, 872–881 (2014).
- [10] SABOORI, A., CHEN, X., BADINI, C., FINO, P. & PAVESE, M. Reactive spontaneous infiltration of Al-activated TiO<sub>2</sub> by molten aluminium. *Trans. Nonferrous Met. Soc. China* 29, 657–666 (2019).
- [11] Salur, E., Aslan, A., Kuntoglu, M., Gunes, A. & Sahin, O. S. Experimental study and analysis of machinability characteristics of metal matrix composites during drilling. *Compos. Part B Eng.* 166, 401–413 (2019).
- [12] Liu, L., Li, W., Tang, Y., Shen, B. & Hu, W. Friction and wear properties of short carbon fibre reinforced aluminium matrix composites. *Wear* 266, 733–738 (2009).
- [13] Moustafa, S. ., El-Badry, S. ., Sanad, A. . & Kieback, B. Friction and wear of copper–graphite composites made with Cu-coated and uncoated graphite powders. *Wear* 253, 699–710 (2002).
- [14] Li, X., Wang, X., Zhang, L., Lee, S., & Dai, H. (2008). Chemically derived, ultrasoft graphene nanoribbon semiconductors. *Science*, 319(5867), 1229-1232.
- [15] Rafiee, M. A., Rafiee, J., Wang, Z., Song, H., Yu, Z. Z., & Koratkar, N. (2010). Enhanced mechanical properties of nanocomposites at low graphene content. *ACS nano*, 4(12), 7415-7420.
- [16] Wang, G., Shen, X., Wang, B., Yao, J., & Park, J. (2009). Synthesis and characterisation of hydrophilic and organophilic graphene nanosheets. *Carbon*, 47(5), 1359-1364.
- [17] Zhang, H., Yu, X., & Braun, P. V. (2010). Three-dimensional bicontinuous ultrafast-charge and-discharge bulk battery electrodes. *Nature Nanotechnology*, 6(5), 277-281.
- [18] Zheng R, Hao X, Yuan Y, Wang Z, Ameyama K, Ma C (2013) Effect of high volume fraction of B<sub>4</sub>C particles on the microstructure and mechanical properties of aluminum alloy based composites. *J Alloy Comp* 576:291–298. <https://doi.org/10.1016/j.jallcom.2013.04.141>
- [19] Rashad M, Pan F, Tang A, Asif M (2014) Effect of graphene nanoplatelets addition on mechanical properties of pure aluminum using a semi-powder method. *Prog Nat Sci Mater Int* 24:101–108. <https://doi.org/10.1016/j.pnsc.2014.03.012>
- [20] Archard JF (1953) Contact and rubbing of flat surfaces. *J Appl Phys* 24:981–988. <https://doi.org/10.1063/1.172144>
- [21] Sekhar R, Singh TP (2015) Mechanisms in turning of metal matrix composites: a review. *J Mater Res Technol* 4:197–207. <https://doi.org/10.1016/j.jmrt.2014.10.013>
- [22] Zhang C, Yao D, Yin J, Zuo K, Xia Y, Liang H, Zeng Y (2019) Effects of  $\beta$ -Si<sub>3</sub>N<sub>4</sub> whiskers addition on mechanical properties and tribological behaviors of Al matrix composites. *Wear* 430–431:145–156. <https://doi.org/10.1016/j.wear.2019.05.003>
- [23] Liu ZY, Wang QZ, Xiao BL, Ma ZY (2010) Clustering model on the tensile strength of PM processed SiCp/Al composites. *Compos Appl Sci Manuf* 41:1686–1692. <https://doi.org/10.1016/j.compositesa.2010.08.007>
- [24] Bastwros MH, Esawi AMK, Wafi A (2013) Friction and wear behaviour of Al–CNT composites. *Wear* 307:164–173. <https://doi.org/10.1016/j.wear.2013.08.021>

DOI: <https://doi.org/10.15379/ijmst.v10i1.3809>

This is an open access article licensed under the terms of the Creative Commons Attribution Non-Commercial License (<http://creativecommons.org/licenses/by-nc/3.0/>), which permits unrestricted, non-commercial use, distribution and reproduction in any medium, provided the work is properly cited.